

Forcing, feedbacks and climate sensitivity in CMIP5 coupled atmosphere-ocean climate models

Timothy Andrews,¹ Jonathan M. Gregory,^{1,2} Mark J. Webb,¹ and Karl E. Taylor³

Received 6 March 2012; revised 11 April 2012; accepted 11 April 2012; published 15 May 2012.

[1] We quantify forcing and feedbacks across available CMIP5 coupled atmosphere-ocean general circulation models (AOGCMs) by analysing simulations forced by an abrupt quadrupling of atmospheric carbon dioxide concentration. This is the first application of the linear forcing-feedback regression analysis of Gregory et al. (2004) to an ensemble of AOGCMs. The range of equilibrium climate sensitivity is 2.1–4.7 K. Differences in cloud feedbacks continue to be important contributors to this range. Some models show small deviations from a linear dependence of top-of-atmosphere radiative fluxes on global surface temperature change. We show that this phenomenon largely arises from shortwave cloud radiative effects over the ocean and is consistent with independent estimates of forcing using fixed sea-surface temperature methods. We suggest that future research should focus more on understanding transient climate change, including any time-scale dependence of the forcing and/or feedback, rather than on the equilibrium response to large instantaneous forcing. **Citation:** Andrews, T., J. M. Gregory, M. J. Webb, and K. E. Taylor (2012), Forcing, feedbacks and climate sensitivity in CMIP5 coupled atmosphere-ocean climate models, *Geophys. Res. Lett.*, 39, L09712, doi:10.1029/2012GL051607.

1. Introduction

[2] Equilibrium climate sensitivity (ECS) is defined as the global equilibrium surface-air-temperature change in response to instantaneous doubling of atmospheric CO₂ concentration. Although this is clearly not a realistic scenario, ECS is a convenient way of quantifying the joint effect of forcing and feedback, which are separately quantities of practical interest for understanding and predicting transient climate change. ECS is thus a useful metric for comparing the response of different climate models [e.g., Knutti and Hegerl, 2008].

[3] Recently, a new generation of climate models, participating in the Coupled Model Intercomparison Project phase 5 (CMIP5), has been developed. Diagnosing the forcings, feedbacks and ECS in each of these models is a first step to identifying and understanding sources of uncertainty in their climate projections.

[4] Feedbacks and ECS have traditionally been estimated from the equilibrium response, which is most easily achieved by replacing the 3D ocean component in an AOGCM with a simple thermodynamic mixed-layer (or ‘slab-ocean’) model. However, the feedbacks in a slab-ocean climate model can be quite different from its AOGCM counterpart that is used for time-dependent historical simulations and climate projections [Williams et al., 2008]. For example, slab-ocean models suppress changes in ocean heat transport which may be important for the pattern of surface warming and atmospheric feedbacks [Boer and Yu, 2003]. In addition, sea-ice schemes can be quite sensitive to ocean processes that are not represented in slab-ocean models [Johns et al., 2006]. Experiments with slab-ocean climate models are not included in the CMIP5 design [Taylor et al., 2012]. Alternative techniques are therefore needed in order to estimate and compare the forcings, feedbacks and ECS of CMIP5 AOGCMs.

[5] Here we apply the method of Gregory et al. [2004] to an ensemble of AOGCMs for the first time. The method is based on a relationship governing the energy balance of the climate system. In order to restore radiative equilibrium, the climate responds to a radiative perturbation F (W m⁻²) with a change in net top-of-atmosphere (TOA) radiative flux N (W m⁻²), which is approximately linearly dependent on global-mean surface-air-temperature change ΔT (K), such that,

$$N = F - \alpha \Delta T, \quad (1)$$

where $-\alpha$ (W m⁻² K⁻¹) is the ‘climate feedback parameter’. If F and α are constant, N is a linear function of ΔT with a slope $-\alpha$ and intercept (at $\Delta T = 0$) of F ; thus both forcing and feedback can be diagnosed by linear regression using this method. The equilibrium temperature change, ΔT_{eqm} , can be estimated by extrapolating this heat balance to equilibrium, that is, $N = 0$ and $\Delta T_{eqm} = F/\alpha$. If the forcing is doubled CO₂, ΔT_{eqm} is the ECS by definition.

[6] An advantage of this method is that the ECS can be estimated from the model response without it actually being run to equilibrium. On the other hand, to make this estimate, we must assume linearity is a good approximation at all times, which may not hold for all models (Section 4). Li et al. [2012] have investigated this question for one model in particular, the ECHAM5/MPIOM model, which they ran in coarse-resolution to equilibrium (~6000 yrs) under 4xCO₂. They found the estimated ΔT_{eqm} using a Gregory approach was within 10% of the actual ΔT_{eqm} , despite some non-linearity.

[7] In this paper we estimate F , $-\alpha$ and ECS in 15 CMIP5 models by applying this method to the abrupt CO₂

¹Met Office Hadley Centre, Exeter, UK.

²NCAS-Climate, University of Reading, Reading, UK.

³Lawrence Livermore National Laboratory, Livermore, California, USA.

Corresponding author: T. Andrews, Met Office Hadley Centre, FitzRoy Road, Exeter EX1 3PB, UK. (timothy.andrews@metoffice.gov.uk)

Published in 2012 by the American Geophysical Union.

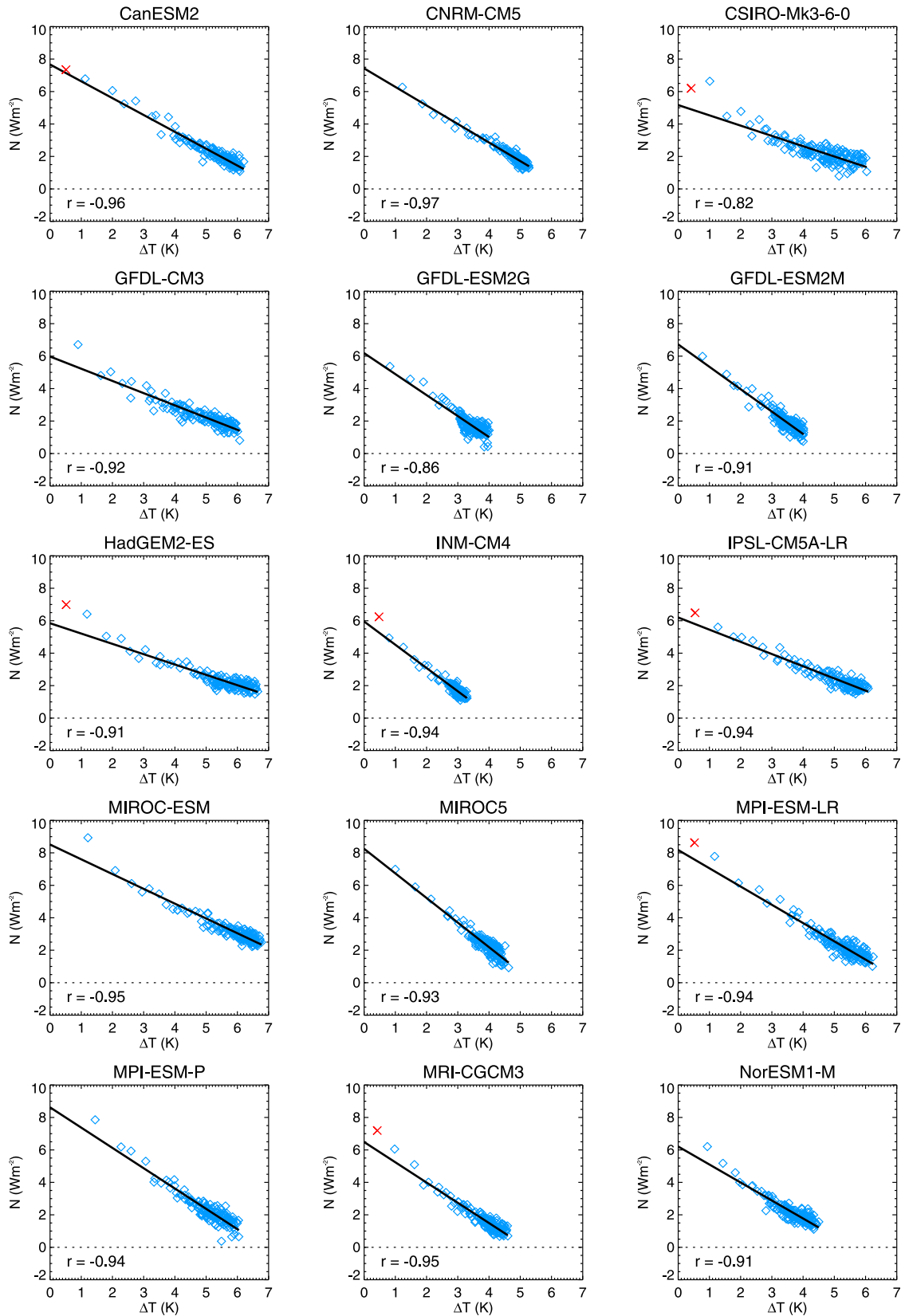


Figure 1. Relationships between the change in net top-of-atmosphere radiative flux, N , and global-mean surface-air-temperature change, ΔT , after an instantaneous quadrupling of CO_2 . Data points are global-annual-means. Lines represent ordinary least squares regression fits to 150 years of data (correlation coefficients, r , are shown). The intercept at $\Delta T = 0$ gives the adjusted radiative forcing, F . The slope of the curve, $-\alpha$, measures the strength of the feedbacks in the climate system, the ‘climate feedback parameter’. The intercept at $N = 0$ gives the equilibrium ΔT , which can alternatively be estimated by F/α . Red crosses represent an independent estimation of the $4\times\text{CO}_2$ adjusted radiative forcing from fixed-SST experiments.

Table 1. Forcing, Feedback and Equilibrium Climate Sensitivity Values^a

AOGCM	Radiative Forcing (Wm^{-2})		Climate Feedback Parameter $-\alpha$ ($\text{Wm}^{-2} \text{K}^{-1}$)				2xCO ₂ Eqm Climate Sensitivity (K)
	Fixed-SST	Regression	Net	LW Clear-Sky	SW Clear-Sky	Net CRE	
CanESM2	7.35	7.67	-1.04	-1.88	0.71	0.13	3.69
CNRM-CM5	n.a.	7.43	-1.14	-1.73	0.78	-0.20	3.25
CSIRO-Mk3-6-0	6.20	5.17	-0.63	-1.70	0.84	0.23	4.08
GFDL-CM3	n.a.	5.98	-0.75	-1.94	0.70	0.48	3.97
GFDL-ESM2G	n.a.	6.18	-1.29	-1.65	0.61	-0.26	2.39
GFDL-ESM2M	n.a.	6.72	-1.38	-1.63	0.58	-0.33	2.44
HadGEM2-ES	6.99	5.85	-0.64	-1.66	0.65	0.37	4.59
INM-CM4	6.24	5.95	-1.43	-1.98	0.67	-0.12	2.08
IPSL-CM5A-LR	6.49	6.20	-0.75	-1.99	0.53	0.70	4.13
MIROC-ESM	n.a.	8.51	-0.91	-1.93	0.83	0.19	4.67
MIROC5	n.a.	8.25	-1.52	-1.85	0.84	-0.51	2.72
MPI-ESM-LR	8.63	8.18	-1.13	-1.79	0.71	-0.04	3.63
MPI-ESM-P	n.a.	8.62	-1.25	-1.80	0.65	-0.10	3.45
MRI-CGCM3	7.19	6.49	-1.25	-1.99	0.83	-0.09	2.60
NorESM1-M	n.a.	6.21	-1.11	-1.86	0.86	-0.11	2.80
Model mean	7.01	6.89	-1.08	-1.83	0.72	0.02	3.37
Standard Dev.	0.85	1.12	0.29	0.13	0.11	0.32	0.83

^aThe 4xCO₂ adjusted radiative forcing has been diagnosed via two independent methods: regression and fixed-SST. The $-\alpha$ and equilibrium climate sensitivity values are derived from ordinary least-squares regression (see text). Uncertainties in the regression fits are indicated in Figure 2.

quadrupling experiments that are core to the CMIP5 experimental design [Taylor *et al.*, 2012].

2. Method

2.1. Climate Model Data

[8] Climate model output was obtained from the CMIP5 multi-model data archive (<http://cmip-pcmdi.llnl.gov/cmip5/index.html>). We use four experiments: piControl (pre-industrial fully-coupled control, run for hundreds of years), abrupt4xCO₂ (as piControl but run for 150 years after instantaneous quadrupling of atmospheric CO₂), sstClim (as piControl but run for 30 years with the ocean and sea-ice models replaced with climatological values, derived from the piControl run, for sea-surface temperature (SST) and sea-ice) and sstClim4xCO₂ (as sstClim but with atmospheric levels of CO₂ instantaneously quadrupled). We extracted monthly mean data for all models available on 15th February 2012, and computed global annual means. We calculate differences between the abrupt4xCO₂ and piControl experiments by subtracting a linear fit of the corresponding control timeseries from the perturbation run, removing any model drift without adding control noise.

[9] It might be questioned whether results derived from experiments with such large abrupt forcing as 4xCO₂ will apply to more realistic transient scenarios, in which the climate system is always closer to equilibrium. We think that strong evidence in support of their applicability is given by Good *et al.* [2011], who showed that the response to a 1% per year compound increase in CO₂ could be constructed from a linear summation of delayed and scaled-down 4xCO₂ responses, implying a consistent behaviour of the simulated climate system under these two very different scenarios.

2.2. Estimating F , α and ECS

[10] We derive our best estimates of $-\alpha$ (slope) and F (intercept) through ordinary least squares regression of global-annual-mean N against ΔT for all 150 data points after CO₂ quadrupling (equation (1) and Figure 1). Note that with this method, F includes rapid adjustments that modify the TOA radiative flux on timescales shorter than a year or

so. Thus, F is referred to as ‘adjusted radiative forcing’ as it includes both stratospheric and tropospheric/land-surface adjustment [Gregory and Webb, 2008; Andrews *et al.*, 2011]. Because CO₂ is quadrupled (rather than doubled), ECS is estimated as $\Delta T_{eqm}/2 = F/2\alpha$.

2.3. Uncertainties

[11] We assess the uncertainty associated with our estimates of F , α and ECS by constructing 95% (2.5–97.5%) confidence intervals through bootstrapping methods. We randomly sample, with replacement, 150 data points from the original dataset to create 10,000 subsets, computing the required term each time. We then sort the resulting distribution to create the 2.5–97.5% confidence interval.

3. Forcing, Feedbacks and ECS

[12] The ECS of each model is given in Table 1 and shown in Figure 2, increasing from left to right. Based on the available CMIP5 model simulations, the ECS spans the range from 2.1 K to 4.7 K, which is similar to the 2.1–4.4 K range diagnosed from equilibrium 2xCO₂ slab-ocean experiments performed with the earlier CMIP3 generation of models [Randall *et al.*, 2007].

[13] There are some differences in F across models (Table 1 and Figure 2), which might be expected from differences in their treatment of radiative transfer [e.g., Collins *et al.*, 2006] and differences across models in rapid tropospheric and land surface adjustment processes [Gregory and Webb, 2008; Andrews and Forster, 2008]. In the previous generation of models, differences in feedbacks contributed more to the uncertainty in ECS than forcing [Webb *et al.*, 2006]. This also appears to be the case in CMIP5. Fixing α at the multi-model mean ($\alpha_{avg} = 1.08 \text{ W m}^{-2} \text{ K}^{-1}$) yields an ECS range of 2.4 to 4.0 K due to differences in F (calculated from $F/2\alpha_{avg}$, using minimum and maximum values of F). Analogously, fixing F at the multi-model mean ($F_{avg} = 6.89 \text{ W m}^{-2}$) gives rise to a substantially larger range of 2.3 K to 5.5 K, due to differences in α . That this is larger than the actual ECS range implies an anti-correlation between forcing and feedbacks across models. Kiehl [2007]

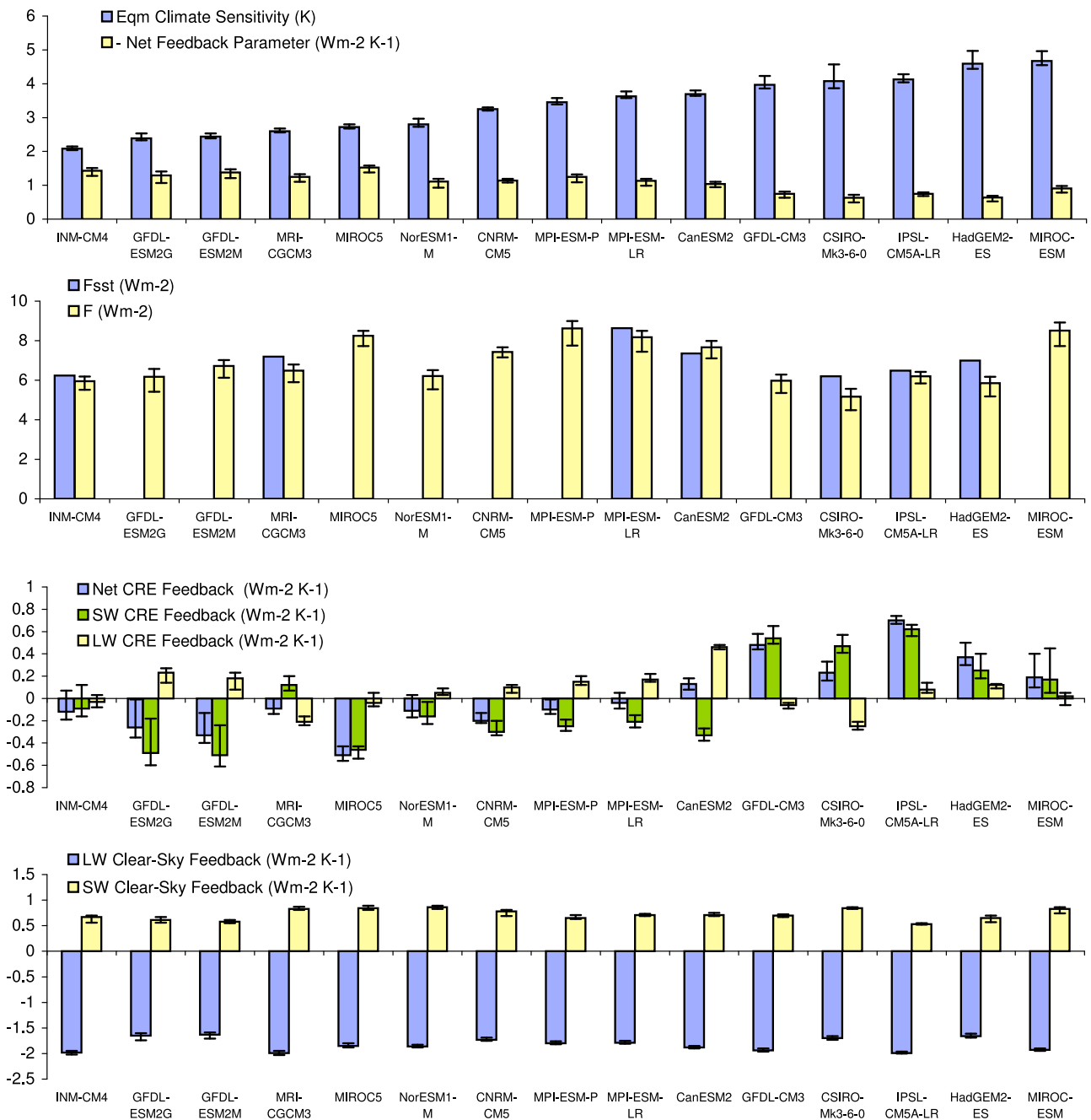


Figure 2. Comparison of the $2\times\text{CO}_2$ equilibrium climate sensitivity, $4\times\text{CO}_2$ adjusted radiative forcing (from fixed-SST, F_{sst} , and regression, F) and various climate feedback terms. The models are ordered from left to right in order of their equilibrium climate sensitivity. Note that in the top panel, α is reported as the climate feedback parameter, rather than $-\alpha$, to maintain the same scale. Errors bars represent 95% (2.5–97.5%) confidence interval on the fit (see Section 2.3).

noted a similar relationship between total anthropogenic forcing and climate sensitivity in the CMIP3 models. In our results, which are for CO_2 -only forcing, the correlation coefficient between F and $-\alpha$ is -0.41 , which is not significant at the 95% level.

[14] Using the same linear regression technique, we decompose the feedback parameter α into longwave (LW) clear-sky, shortwave (SW) clear-sky, and LW and SW cloud radiative effect (CRE) components (all fluxes defined as

positive downwards). For two of the AOGCMs, regression plots are shown in Figure 3 (all models are shown in Figures S1–S6 in the auxiliary material).¹ CRE terms are defined as the difference between all-sky (i.e., with clouds if present) and clear-sky (i.e., clouds artificially removed) net downward

¹Auxiliary materials are available in the HTML. doi:10.1029/2012GL051607.

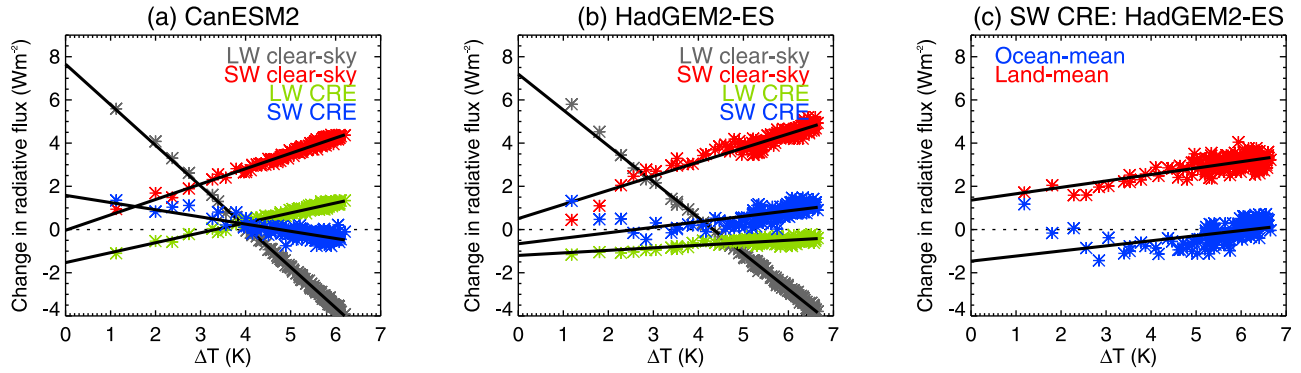


Figure 3. Relationship between the change in global-annual-mean radiative fluxes and global-annual-mean surface-air-temperature change, ΔT , after an instantaneous quadrupling of CO_2 , for (a) a model (CanESM2) that exhibits quite linear behaviour in Figure 1, and (b) a model (HadGEM2-ES) that in the early years exhibits small deviations from linearity. (c) Change in annual-mean SW CRE averaged over land and ocean regions separately, as a function of ΔT , in HadGEM2-ES. All fluxes are positive downwards. Lines represent ordinary least squares regression fits to 150 years of data.

radiative fluxes. This term is sometimes referred to as ‘cloud radiative forcing’ (CRF) in the literature. Note that changes in CRE should not be interpreted as being due to changes in cloud properties alone since the masking effects of clouds on clear-sky fluxes also contribute [e.g., Soden *et al.*, 2008].

[15] There is good agreement (Figure 2 and Table 1) across models in strongly negative (stabilizing) LW clear-sky feedback processes (range is -1.6 to $-2.0 \text{ Wm}^{-2} \text{ K}^{-1}$), which comes about principally due to the Planck response, partly offset by a positive (destabilizing) contribution due to the net effect of the water-vapour and lapse-rate feedbacks. There is also good agreement in the sign (positive) and strength (range is 0.5 to $0.9 \text{ Wm}^{-2} \text{ K}^{-1}$) of SW clear-sky feedback. This feedback is largely due to a retreat of snow cover and sea-ice with warming and the SW contribution of the water-vapour feedback, which together decrease the planetary albedo, thereby enhancing the amount of absorbed solar radiation.

[16] Larger differences between models emerge when we look at the response of clouds. The multi-model mean CRE feedback is close to zero (Table 1). However, the models span a wide range (-0.5 to $+0.7 \text{ Wm}^{-2} \text{ K}^{-1}$), which explains most of the range in the net feedback parameter, as in CMIP3 [Ringer *et al.*, 2006]. Soden *et al.* [2008] showed that cloud feedback is either near neutral or positive in all CMIP3 models when changes in CRE are adjusted for cloud masking effects. Our most negative CRE feedback ($-0.5 \text{ Wm}^{-2} \text{ K}^{-1}$) falls within their CRE range. Hence we find no reason to doubt that their result will also hold for the CMIP5 models. When ordered by increasing ECS (Figure 2), it is clear that the spread of ECS can to a certain extent be explained by differences in CRE feedbacks, i.e., those models with a more positive CRE feedback tend to have a larger ECS. As with the older generation models [Webb *et al.*, 2006], this spread mostly comes from differences in SW CRE feedback processes (Figure 2).

[17] We use the CMIP5 experiments with fixed SSTs (sstClim and sstClim4xCO2, described in Section 2.1) to derive an alternative estimate of the adjusted radiative forcing [Shine *et al.*, 2003; Hansen *et al.*, 2005], which we denote by $F_{SS\text{T}}$. In these experiments the atmosphere and

land surface are free to respond to changes in CO_2 but the SSTs, and as a result climate feedbacks, are prevented from evolving. Thus, $\Delta T \sim 0$ and $F = N$ according to equation (1). $F_{SS\text{T}}$ is therefore calculated from a time averaged N (30 year mean of the net TOA radiative flux, after removing any flux imbalance found in the control).

[18] Differences between F and $F_{SS\text{T}}$ in the models with available data are generally small (Figure 2); the correlation coefficient between F and $F_{SS\text{T}}$ is 0.89. Exact agreement is not expected due to the different ways in which the methods impose $\Delta T = 0$. Land temperatures can, for example, respond in fixed SST experiments. This gives rise to a small global ΔT increase (Figure 1) and may cause circulation changes and other responses that affect the radiation balance. With the regression method however, $\Delta T = 0$, but local temperatures are unconstrained everywhere.

4. Non-linear Responses

[19] Figure 1 shows that a linear relationship between N and ΔT is a good approximation (correlation coefficients are greater than 0.9 in most cases), at least under the level of forcing and timescale considered here. There are, however, small deviations from linear behaviour in some models that demand further consideration. In the first year, for example, N tends to fall above the regression line. This is evident in eight of the models (CSIRO-Mk3-6-0, HadGEM2-ES, MIROC-ESM, MPI-ESM-LR, MPI-ESM-P, MRI-CGCM3, NorESM1-M and GFDL-CM3). Consistent with this initial evolution, $F_{SS\text{T}}$ also falls above the regression line.

[20] We examine this behaviour in more detail using the decomposition into LW and SW clear-sky and CRE components (Figures 3a and 3b). In all models, the clear-sky and LW CRE fluxes are largely linear with ΔT , with only small deviations. The single largest contributor to the non-linear behaviour is the SW CRE component (Figures 3b and S6). Averaging the SW CRE response over land and ocean regions separately shows that this principally results from a non-linear response over the ocean, not seen over land (Figures 3c and S7).

[21] What processes could give rise to these deviations from linear behaviour? Consistent with an initial non-linear CRE response over the ocean, *Williams et al.* [2008] described a delayed SST warming and stratocumulus cloud response on the eastern side of the tropical ocean basins for the first few decades after CO₂ doubling in an older generation model. A different pattern of surface warming can give rise to a different TOA radiative flux change for the same global-mean ΔT , particularly from clouds [e.g., *Williams et al.*, 2008; *Senior and Mitchell*, 2000].

[22] If the non-linear behaviour is confined to the first decade or so, then the curvature can be expressed as a decadal adjustment to F [*Williams et al.*, 2008]. On the other hand, a time-varying α would be a more appropriate description if the non-linearity depends on the evolution of the ocean mixed layer and the pattern of SST [*Winton et al.*, 2010]. Non-linear behaviour may also exist on even longer time scales if changes in the state of the deep ocean influence the pattern of surface warming and atmospheric feedbacks, especially in the Southern Ocean [*Held et al.*, 2010; *Li et al.*, 2012; *Senior and Mitchell*, 2000].

5. Summary and Discussion

[23] We have evaluated the ECS of a subset of available CMIP5 models and compared the forcing and feedbacks that jointly determine it. Unlike previous assessments where equilibrium slab-ocean experiments were used to determine ECS, the CMIP5 experiments included fully coupled AOGCM runs forced by an abrupt quadrupling of CO₂ from which ECS can be diagnosed. Here then for the first time we were able to apply the *Gregory et al.* [2004] methodology to a multi-model ensemble of AOGCMs. Results show that the range of ECS has not decreased relative to previous generations of models and that differences in cloud feedback continue to be the largest, but not the only, source of this uncertainty.

[24] We find that a linear relationship between N and ΔT is a good approximation under the level of forcing and time-scales considered here. There are however, small deviations from linear behaviour in some models. In these cases, N in the first year falls above the regression line (based on all data, equally weighted), consistent with independent estimates of forcing derived using fixed-SST experiments. We identify changes in SW CRE over oceans as the largest contributor to the non-linear behaviour.

[25] If substantial non-linear responses were found to exist on timescales longer than the 150 years of the abrupt4xCO₂ experiments, a linear forcing-feedback framework would be inadequate. When the behaviour is non-linear, the distinction between forcing and feedback is not well-defined, and it is arbitrary whether the non-linearity is interpreted as a varying forcing or a varying feedback or both. One possible characterisation is an adjusted radiative forcing and a time-evolving feedback parameter, which could be defined as the tangent to the curve [*Gregory et al.*, 2004], i.e., dN/dT .

[26] In AOGCMs showing non-linearity, estimating equilibrium climate change clearly becomes less reliable, calling into question whether ECS is still useful as a means of quantifying and understanding responses to external forcing. We suggest that improved understanding of climate

responses on various timescales [e.g., *Williams et al.*, 2008; *Held et al.*, 2010; *Watanabe et al.*, 2011; *Li et al.*, 2012] should be a priority if we want to progress beyond the limitations of the linear forcing-feedback paradigm and thus improve our understanding of transient climate change, as well its relationship to the equilibrium response.

[27] **Acknowledgments.** This work was supported by the Joint DECC/Defra Met Office Hadley Centre Climate Programme (GA01101) and (for JMG) by the NCAS-Climate programme. Two reviewers helped improve the clarity of the paper. We acknowledge the World Climate Research Programme's Working Group on Coupled Modelling, which is responsible for CMIP, and we thank the climate modelling groups (listed in Table 1 of this paper) for producing and making available their model output. For CMIP the U.S. Department of Energy's Program for Climate Model Diagnosis and Intercomparison provides coordinating support and led development of software infrastructure in partnership with the Global Organization for Earth System Science Portals. The U.S. DOE also supported work by KET through its Regional and Global Climate Modeling Program.

[28] The Editor thanks Alex Jonko and an anonymous reviewer for assisting with the evaluation of this paper.

References

- Andrews, T., and P. M. Forster (2008), CO₂ forcing induces semi-direct effects with consequences for climate feedback interpretations, *Geophys. Res. Lett.*, *35*, L04802, doi:10.1029/2007GL032273.
- Andrews, T., J. M. Gregory, P. M. Forster, and M. J. Webb (2011), Cloud adjustment and its role in CO₂ radiative forcing and climate sensitivity: A review, *Surv. Geophys.*, doi:10.1007/s10712-011-9152-0.
- Boer, G. J., and B. Yu (2003), Dynamical aspects of climate sensitivity, *Geophys. Res. Lett.*, *30*(3), 1135, doi:10.1029/2002GL016549.
- Collins, W. D., et al. (2006), Radiative forcing by well-mixed greenhouse gases: Estimates from climate models in the Intergovernmental Panel on Climate Change (IPCC) Fourth Assessment Report (AR4), *J. Geophys. Res.*, *111*, D14317, doi:10.1029/2005JD006713.
- Good, P., J. M. Gregory, and J. A. Lowe (2011), A step-response simple climate model to reconstruct and interpret AOGCM projections, *Geophys. Res. Lett.*, *38*, L01703, doi:10.1029/2010GL045208.
- Gregory, J. M., and M. J. Webb (2008), Tropospheric adjustment induces a cloud component in CO₂ forcing, *J. Clim.*, *21*, 58–71, doi:10.1175/2007JCLI1834.1.
- Gregory, J. M., W. J. Ingram, M. A. Palmer, G. S. Jones, P. A. Stott, R. B. Thorpe, J. A. Lowe, T. C. Johns, and K. D. Williams (2004), A new method for diagnosing radiative forcing and climate sensitivity, *Geophys. Res. Lett.*, *31*, L03205, doi:10.1029/2003GL018747.
- Hansen, J., et al. (2005), Efficacy of climate forcings, *J. Geophys. Res.*, *110*, D18104, doi:10.1029/2005JD005776.
- Held, I. M., et al. (2010), Probing the fast and slow components of global warming by returning abruptly to preindustrial forcing, *J. Clim.*, *23*, 2418–2427, doi:10.1175/2009JCLI3466.1.
- Johns, T. C., et al. (2006), The new Hadley Centre climate model Had-GEM1: Evaluation of coupled simulations, *J. Clim.*, *19*, 1327–1353, doi:10.1175/JCLI3712.1.
- Kiehl, J. T. (2007), Twentieth century climate model response and climate sensitivity, *Geophys. Res. Lett.*, *34*, L22710, doi:10.1029/2007GL031383.
- Knutti, R., and G. C. Hegerl (2008), The equilibrium sensitivity of the Earth's temperature to radiation changes, *Nat. Geosci.*, *1*, 735–743, doi:10.1038/ngeo337.
- Li, C., J.-S. V. Storch, and J. Marotzke (2012), Deep-ocean heat uptake and equilibrium climate response, *Clim. Dyn.*, doi:10.1007/s00382-012-1350-z.
- Randall, D. A., et al. (2007), Climate models and their evaluation, in *Climate Change 2007: The Physical Science Basis. Contribution of Working Group I to the Fourth Assessment Report of the Intergovernmental Panel on Climate Change*, edited by S. Solomon et al., pp. 591–662, Cambridge Univ. Press, Cambridge, U. K.
- Ringer, M. A., et al. (2006), Global mean cloud feedbacks in idealized climate change experiments, *Geophys. Res. Lett.*, *33*, L07718, doi:10.1029/2005GL025370.
- Senior, C. A., and J. F. B. Mitchell (2000), The time-dependence of climate sensitivity, *Geophys. Res. Lett.*, *27*(17), 2685–2688, doi:10.1029/2000GL011373.
- Shine, K. P., J. Cook, E. J. Highwood, and M. J. Joshi (2003), An alternative to radiative forcing for estimating the relative importance of climate

- change mechanisms, *Geophys. Res. Lett.*, *30*(20), 2047, doi:10.1029/2003GL018141.
- Soden, B. J., et al. (2008), Quantifying climate feedbacks using radiative kernels, *J. Clim.*, *21*, 3504–3520, doi:10.1175/2007JCLI2110.1.
- Taylor, K. E., R. J. Stouffer, and G. A. Meehl (2012), An overview of CMIP5 and the experiment design, *Bull. Am. Meteorol. Soc.*, *90*, 485–498, doi:10.1175/BAMS-D-11-00094.1.
- Watanabe, M., et al. (2011), Fast and slow timescales in the tropical low-cloud response to increasing CO₂ in two climate models, *Clim. Dyn.*, doi:10.1007/s00382-011-1178-y.
- Webb, M. J., et al. (2006), On the contribution of local feedback mechanisms to the range of climate sensitivity in two GCM ensembles, *Clim. Dyn.*, *27*, 17–38, doi:10.1007/s00382-006-0111-2.
- Williams, K. D., W. J. Ingram, and J. M. Gregory (2008), Time variation of effective climate sensitivity in GCMs, *J. Clim.*, *21*, 5076–5090, doi:10.1175/2008JCLI2371.1.
- Winton, M., K. Takahashi, and I. M. Held (2010), Importance of Ocean Heat Uptake Efficacy to Transient Climate Change, *J. Clim.*, *23*, 2333–2344, doi:10.1175/2009JCLI3139.1.